Phytopathology Research

RESEARCH Open Access

Wheat root transcriptional responses against *Gaeumannomyces graminis* var. *tritici*

Jie Zhang[1†], Haixia Yan[2†], Mingcong Xia[1], Xiaoyun Han[1], Lihua Xie[3], Paul H. Goodwin[4], Xin Quan[1], Runhong Sun[1], Chao Wu[1] and Lirong Yang[1*]

Abstract

Wheat root rot caused by *Gaeumannomyces graminis* var. *tritici* (*Ggt*) results in severe yield losses in wheat production worldwide. However, little is known about the molecular mechanism that regulates systemic symptom development in infected wheat. Fluorescent microscopy observation of the stained wheat roots infected by *Ggt* showed that lesions were visible when the fungus could be detected in the endodermis, pericycle and phloem at 5 days post inoculation (dpi), and rust symptoms were visible when there was extensive fungal colonization in the root cortex at 6 dpi. Transcriptome sequencing of *Ggt*-inoculated wheat roots and healthy control root samples was performed at 5 dpi to identify *Ggt*-induced gene expression changes in wheat roots at the time of lesion formation. A total of 3973 differentially expressed genes (DEGs) were identified, of which 1004 (25.27%) were up-regulated and 2969 (74.73%) were down-regulated in *Ggt*-inoculated wheat roots compared with those in control roots. GO annotation and KEGG pathway analysis of these DEGs revealed that many of them were associated with pathogen resistance, such as those involved in oxidation-reduction process, tryptophan biosynthesis process, and phenylpropanoid biosynthesis process. Analysis of DEGs revealed that 15 DEGs were involved in cellular regulation, 57 DEGs in signal transduction pathways, and 75 DEGs in cell wall reorganization, and 23 DEGs are pathogenesis-related proteins. Reverse transcription quantitative PCR (RT-qPCR) of 13 of those DEGs showed that these genes may play roles in wheat resistance against *Ggt*. Overall, this study represents the first transcriptional profiling of wheat roots in response to *Ggt* infection and further characterization of DEGs identified in this study may lead to better understanding of resistance against take-all in wheat.

Keywords: *Triticum aestivum* L., *Gaeumannomyces graminis* var. *tritici*, Wheat roots, RNA-Seq, Differentially expressed genes, Plant defense response

Background

Wheat (*Triticum aestivum* L.) is the most extensively grown cereal crop and one of the four major food crops in the world (McMillan et al. 2014). *Gaeumannomyces graminis var. tritici* (*Ggt*), a soil-borne necrotrophic fungal pathogen, causes a root rot disease in wheat known as take-all (Cook 2003; Kwak et al. 2009; Yang et al. 2015a). Runner hyphae of *Ggt* grow along the surface of plant roots and then penetrate their epidermis, spreading through the cortex, endodermis and stele, destroying the phloem and xylem, thus preventing the movement of assimilates, such as water and ions. Eventually the plant becomes stunted and yellowed with white heads developed, which results in reduced wheat production (Cook 2003; Guilleroux and Osbourn 2004). Root rot caused by *Ggt* is one of the most serious

* Correspondence: luck_ylr@126.com
†Jie Zhang and Haixia Yan contributed equally to this work.
[1]Institute of Plant Protection Research, Henan Academy of Agricultural Sciences, Henan Biopesticide Engineering Research Center, Henan International Joint Laboratory of Crop Protection, Zhengzhou 450002, P. R. China
Full list of author information is available at the end of the article

diseases of wheat worldwide, additionally, take-all disease also occurs in rye, barley and other plants belonging to Poaceae (Weller 1988; Weller et al. 2002; Cook 2003).

Plants have a variety of mechanisms to defend themselves against pathogen infections (Mattiacci et al. 1995; Glazebrook 2005; Koornneef and Pieterse 2008). There are significant differences between plant resistance to root pathogens and to foliar pathogens (Mooney et al. 2006; Sang et al. 2010; De Coninck et al. 2015). In the absence of effector recognition by resistance genes, the attacking fungus would be recognized by host plant through its microbe-associated molecular patterns (MAMPs) or damage associated molecular patterns (DAMPs) that result in induction of plant defenses (De Coninck et al. 2015). Several root pathogens are known to evade or suppress this recognition through effector-triggered susceptibility, but effectors of root pathogens can also be recognized, resulting in a type of resistance without activation of the programmed cell death that has been observed in foliar pathogens (De Coninck et al. 2015). In plant root diseases, defense signaling can be mediated by jasmonic acid (JA), ethylene (ET), and salicylic acid (SA) as well as abscisic acid, auxins, cytokinins, gibberellins, brassinosteroids and other signalling molecules, like those in foliar diseases (Browse 2009). However, root defense responses, such as production of pathogenesis-related (PR) proteins, cell wall modifications, reactive oxygen species, and phytoalexins may differ from that in leaves (Bertini et al. 2009; Sherif et al. 2012; De Coninck et al. 2015; Li et al. 2015). Therefore, it is necessary to investigate the responses of plant roots to root pathogens and the corresponding defense mechanisms rather than just rely on results of plant leaves to foliar pathogens.

RNA sequencing (RNA-Seq), a high-throughput and high-resolution sequencing technology, has achieved widespread consideration as an important new tool for transcriptomics analysis (Fang et al. 2015; Yang et al. 2015b), and has recently been applied to uncover the complex responses of plant roots to pathogen infection. For example, using this technique, Shin et al. (2014) examined defense response of apple root against *Pythium ultimum*; Chand et al. (2016) studied turmeric root resistance to *P. aphanidermatum*; Wang et al. (2012) investigated the banana root response to *Fusarium oxysporum* f. sp. *cubense*, and Zuluaga et al. (2015) compared susceptible and resistant responses of wild potato roots inoculated with *Ralstonia solanacearum*.

In this study, RNA-Seq approach was adopted to identify the differentially expressed genes (DEGs) between the pathogen-inoculated wheat roots and healthy control roots at 5 days post inoculation (dpi) with *Ggt* when lesions are first visible on roots. Based on the transcriptome data obtained, this study represents the first transcriptional profiling of wheat roots in response to *Ggt* infection and further characterization of DEGs identified in this study may lead to better understanding of resistance against take-all in wheat.

Results

Impact of *Gaeumannomyces graminis* var. *tritici* inoculation on wheat plants

The leaf length of wheat seedlings infected by *Ggt* was significantly shorter than that of the control starting at 6 dpi (Fig. 1a). After 10 dpi, leaves of the infected wheat appeared chlorotic (data not shown). A significant shorter root length was also observed in *Ggt*-inoculated wheat seedlings compared with control at 3 dpi (Fig. 1b, c). No symptoms were visible on wheat roots infected by the take-all fungus until 5 dpi when the characteristically black to chocolate brown lesions were observed. By comparison, control roots never showed lesions or rust discoloration. The results indicated that root growth was inhibited before visible symptoms appeared, and then inhibition of leaf growth occurred. Also, it takes several days before the fungus produced visible necrosis, even though it is considered a necrotroph rather than a hemibiotroph.

Staining of the *Ggt* -inoculated wheat root tissues with WGA-AF88 resulted in green-stained fungal hyphae, and staining with propidium iodide (PI) resulted in red-stained root tissues (Fig. 2). After infection, *Ggt* hyphae was detected mainly in the root endodermis and pericycle region at 1 dpi, and then in the phloem at 2–5 dpi. Hyphae could be detected extensively in the cortex at 6 and 7 dpi. At 8 dpi, the cortex cells were highly degraded and the endodermis cells were shrunken, and the central xylem vessels were filled with hyphae. Thus, dark brown lesions were observed just prior to the extensive fungal colonization of the cortex, and rust symptoms were observed when a widespread colonization of the cortex by *Ggt* took place.

RNA sequencing and de novo assembly of transcriptome

RNA sequencing of *Ggt*-inoculated and control wheat roots at 5 dpi, the time of the first appearance of necrosis, yielded a total of 35,008,455 (*Ggt*-inoculated) and 62,983,181 (control) raw paired-end reads, and 32,457,257 (*Ggt*-inoculated) and 58,957,023 (control) clean paired-end reads after filtering out low-quality reads and trimming adaptor sequences (Additional file 1: Table S1). The mean of Q20 percentage (proportion of nucleotides with quality value larger than 20 in reads), Q30 percentage (proportion of nucleotides with quality value larger than 30 in reads) and GC percentage are 95.87, 87.95 and 55.46%, respectively. After removal of *Ggt* unigenes, splicing variants, and redundant sequences, 103,368 non-redundant wheat unigenes were obtained.

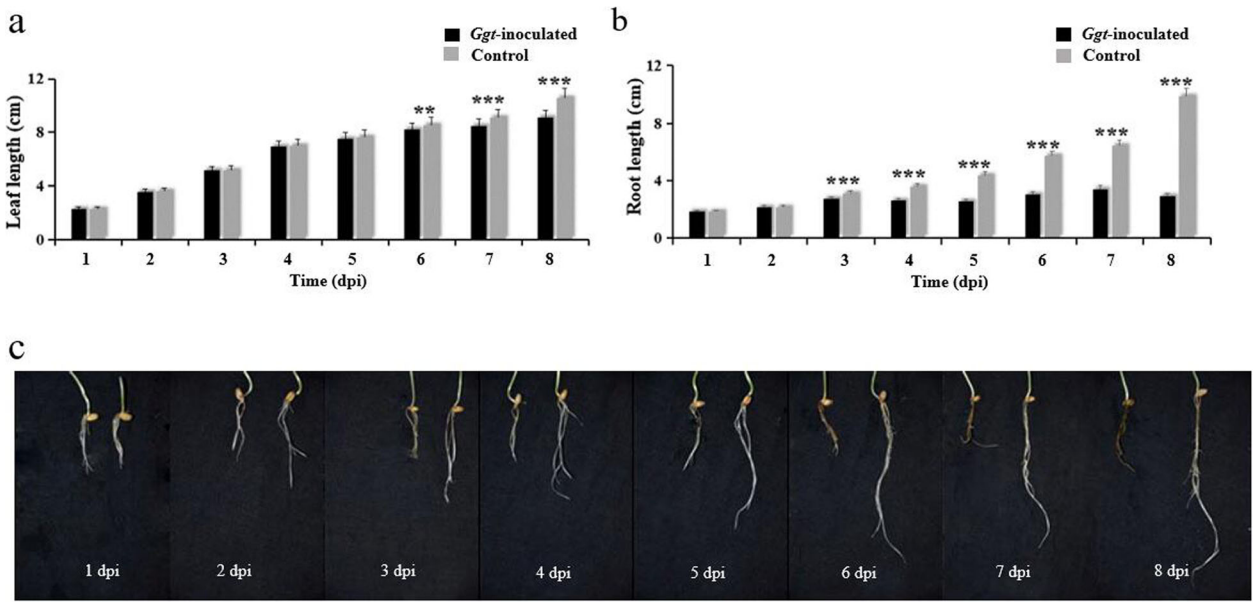

Fig. 1 Growth characteristics of wheat inoculated with *Gaeumannomyces graminis* var. *tritici* over a time course of 8 days. **a** Leaf length of wheat inoculated with *Ggt*. **b** Root length of wheat inoculated with *Ggt*. **c** Images of wheat roots inoculated with *Ggt* (left) and control roots (right). Asterisks indicated a statistically significant differences between *Ggt*-inoculated wheat and wheat (**, $P < 0.005$, ***, $P < 0.0001$) as determined by the Student t-test

Identification and analysis of DEGs in wheat roots during the response to *Ggt* infection

A total of 53,984 wheat unigenes were annotated based on the NCBI nr database. The gene expression levels based on FPKM and gene densities of the *Ggt*-inoculated and control samples were similar (Fig. 3a, b), indicating that the RNA-seq data were reliable. Based on FPKM, 3973 DEGs (with $P < 0.005$ and $|\log_2(\text{fold change})| > 1$) were identified. Among them, 1004 genes displayed up-regulated expression and 2969 genes displayed down-regulated expression in *Ggt*-inoculated roots compared to those in control roots (Fig. 3c). Hierarchical clustering of the 1004 up-regulated DEGs showed that the gene expression pattern could be divided into multiple clusters (Fig. 4a). There were two main clusters, one containing 60 DEGs and the other containing 944 DEGs. Hierarchical clustering of the 2969 down-regulated DEGs showed that the overall gene expression pattern was divided into two broad clusters (Fig. 4b): the large cluster contained 2645 DEGs with relatively low expression levels in both *Ggt*-inoculated and control roots, while the smaller cluster contained 324 DEGs with relatively high expression levels in *Ggt*-inoculated and control roots. In general, DEGs with extremely high or low expression levels (i.e., most intense blue or red in Fig. 4) were more common among down-regulated DEGs, whereas DEGs with medium or slightly higher/lower expression (i.e., white or light blue or red in the figure) were more common in the up-regulated DEGs.

GO analysis of DEGs during the response of wheat roots to *Ggt* infection

GO was used to analyze the functional classifications of the 1004 up-regulated (Fig. 5a), and 2969 down-regulated DEGs (Fig. 5b). The DEGs were first divided based on biological process (BP). The largest BP subcategory for up-regulated DEGs was involved in metabolic process, which comprised 723 DEGs, and the largest BP subcategory for down-regulated DEGs was also related to metabolic process, which comprised 1987 DEGs. Compared with the down-regulated DEGs, there were more up-regulated DEGs that were involved in metabolic processes related to oxoacids, organic acids, cellular amino acids, small molecules, alpha-amino acids, organ nitrogen compounds, L-phenylalanine, erythrose 4-phosphate/phosphoenolpyruvate family amino acids, aromatic amino acid family biosynthesis, cellular biogenic amines, cellular amines, phenylpropanoids, amine biosynthesis, cellular biogenic amine biosynthesis and tryptophan biosynthesis. This indicates a re-orientation of metabolism possibly towards more proteins and secondary compounds including anti-microbial compounds. Meanwhile, compared with the up-regulated DEGs, there were more down-regulated DEGs that were involved in metabolic processes related to ribosome biogenesis, cellular component biogenesis, translation, response to oxidative stress, microtubule-based movement, fatty acid biosynthesis, glucans, cellulose biosynthesis, carbohydrates, monocarboxylic acid biosynthesis,

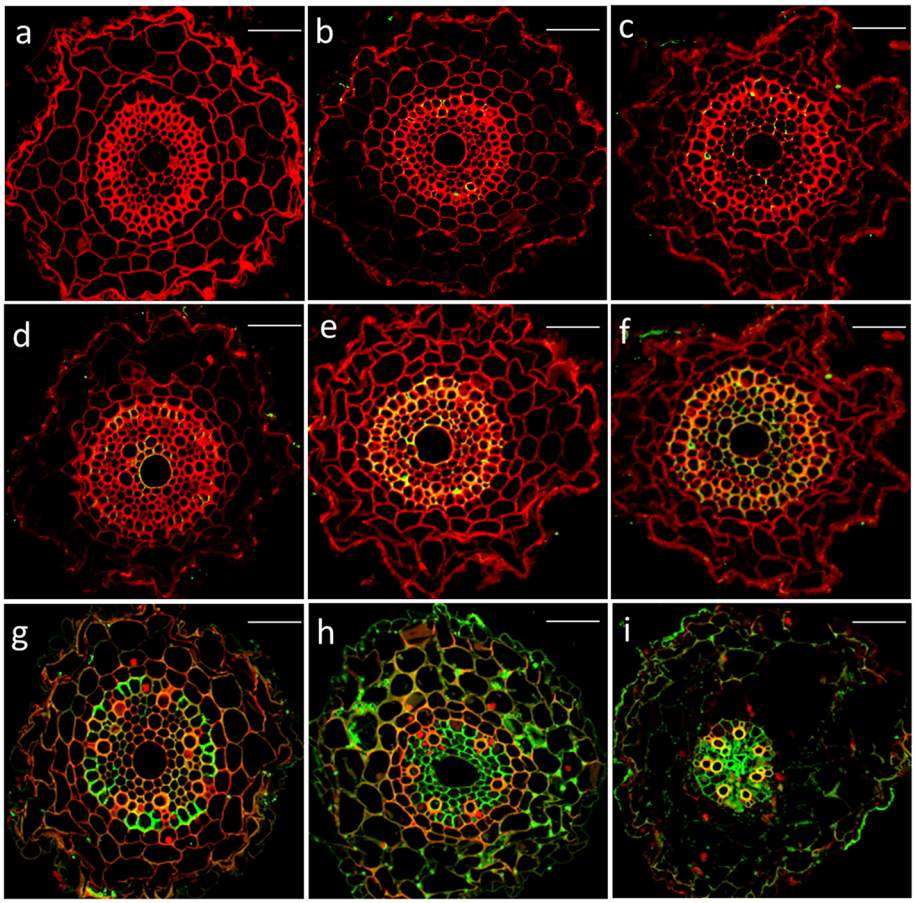

Fig. 2 Wheat roots infected by *Gaeumannomyces graminis* var. *tritici* were stained with WGA-AF488 and PI. **a** Control root at 5 dpi showing that root tissues were stained red. **b**-**i** *Ggt*-inoculated root showing that fungal hyphae were stained green at 1 dpi (**b**), 2 dpi (**c**), 3 dpi (**d**), 4 dpi (**e**), 5 dpi (**f**), 6 dpi (**g**), 7 dpi (**h**) and 8 dpi (**i**). Each bar represents 100 μm

generation of precursor metabolites/energy, nucleotide-sugars and UDP-glucose. This indicates a re-orientation of metabolism possibly towards less generation of sugars and sugar derivatives like cell wall materials and sugar nucleotides, as well as less fatty acids and fewer ribosomes.

The DEGs were next divided based on cellular component (CC) (Fig. 5). For up-regulated DEGs, there was only one CC subcategory, apoplast, which was not observed for the down-regulated DEGs. Of the 19 CC subcategories for down-regulated DEGs, the four largest were intracellular part, cell, cell part and intracellular, which were comprised of 164, 180, 180 and 169 DEGs, respectively. This indicates that up-regulation of DEGs was more oriented towards responses in the apoplast, which is where *Ggt* would be growing in the plant roots. In contrast, down-regulation of DEGs was more oriented towards the cytoplasm where re-orientation of metabolism may have been occurring in response to infection.

Finally, GO analysis was used to divide the DEGs based on molecular function (MF) (Fig. 5). The largest subcategory for up-regulated DEGs among the MF subcategories was related to catalytic activity followed by ion binding, cation binding and metal ion binding, which were comprised of 439, 287, 164, 152 DEGs, respectively. None of those subcategories existed in the down-regulated DEGs. Thus, ion binding appeared to be an important feature up-regulated by *Ggt* infection. The largest MF subcategories for down-regulated DEGs were related to catalytic activity and oxidoreductase activity, which were comprised of 618 and 159 DEGs, respectively. Therefore, there appeared to be a considerable down-regulation of enzyme activity, perhaps also related to a re-orientation of metabolism due to *Ggt* infection.

KEGG pathway analysis of DEGs during the response of wheat roots to *Ggt* infection

Using the KEGG pathway database, 117 biological pathways were identified among the up-regulated DEGs (Additional file 2: Figure S1a). The most enriched KEGG pathways were those related to diterpenoid biosynthesis, isoquinoline alkaloid biosynthesis,

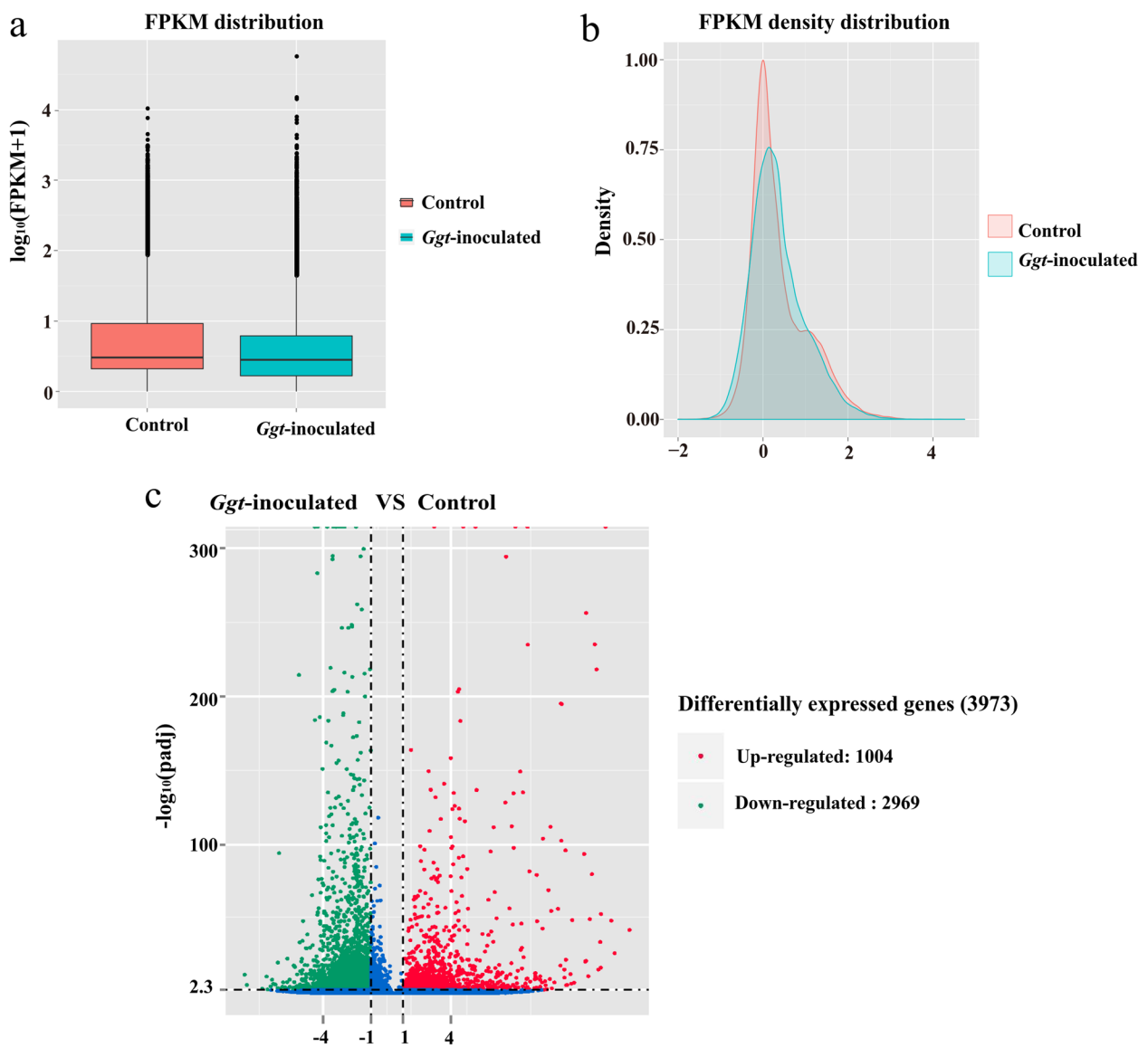

Fig. 3 Gene expression comparisons between *Ggt*-inoculated and control wheat groups, and hierarchical clustering analyses of DEGs. **a** Boxplot showing the overall expression levels of samples. The box represents 50% of the FPKM, and the y-axis corresponds to samples' $\log_{10}$ (FPKM+ 1). **b** FPKM density distribution of samples. The y-axis corresponds to gene density, and the x-axis displays the $\log_{10}$ (FPKM) of samples. **c** Volcano of DEGs between *Ggt*-inoculated and control wheat roots. The y-axis corresponds to the mean expression value of $\log_{10}$ (*p*-value), and the x-axis displays the $\log_2$ fold change value. The red dots represent up-regulated DEGs, and the green dots represent down-regulated DEGs

stilbenoid, diarylheptanoid and gingerol biosynthesis, phenylalanine, tyrosine and tryptophan biosynthesis, and flavonoid biosynthesis, with each pathway containing only 10–20 genes. This indicated that significant changes took place in secondary metabolism in the roots, and some could be related to the production of compounds with antimicrobial activities.

There were 158 enriched KEGG pathways among the down-regulated DEGs (Additional file 2: Figure S1b), of which the ribosomal genes were highly enriched. This agrees well with the GO annotation of the ribosome among the down-regulated DEGs classified based on CC subcategories (Fig. 5b). Other highly enriched down-regulated DEGs were related to linolenic acid metabolism, gap junction, ascorbate and aldarate metabolism, oxidative phosphorylation and phagosome pathways, each having 25 or less DEGs.

Analysis of DEGs involved in defense regulation

Several DEGs related to defense regulation might be involved in the biotic stress response (Table 1). Among them, seven WRKY transcription factors were up-regulated by *Ggt* infection, whereas WRKY transcription factor 35 was down-regulated (Table 1). Three up-

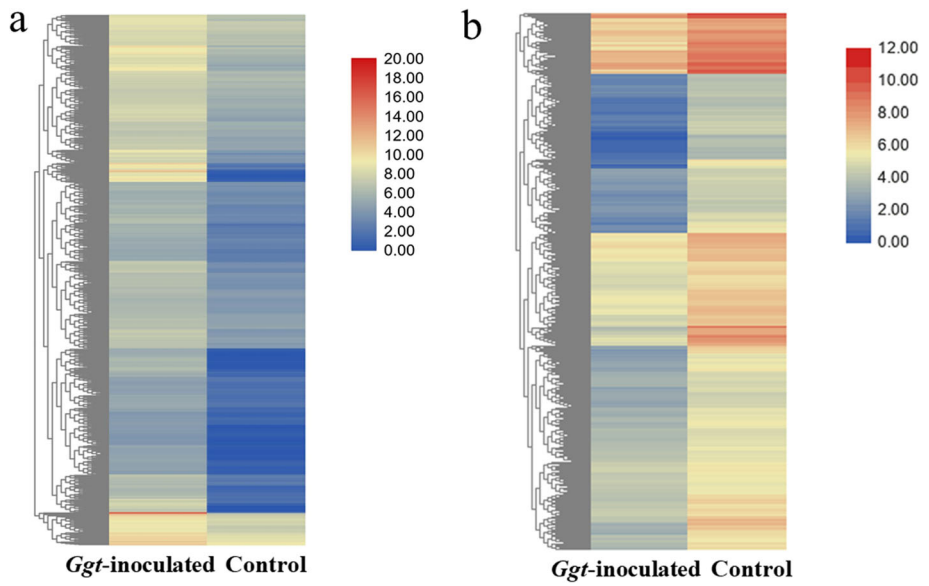

Fig. 4 Hierarchical clustering analysis of DEGs. **a** Hierarchical clustering analysis of up-regulated DEGs. **b** Hierarchical clustering analysis of down-regulated DEGs. The DEGs were clustered based on the $\log_{10}$ (FPKM+ 1). Dark red indicates high expressed genes, dark blue indicates low expressed genes. Color from red to blue denotes the numeric values from large to small

regulated DEGs in *Ggt*-infected wheat were related to the mitogen-activated protein kinase (MAPK) pathway, whereas four MAPK-related DEGs were significantly down-regulated in *Ggt*-inoculated wheat roots compared with control (Table 1).

Analysis of DEGs involved in signal transduction pathways

A number of DEGs were related to calcium, an important signaling molecule. There were four up-regulated and five down-regulated DEGs encoding for calmodulin (CaM) Ca^{2+}-binding proteins, and there were three up-regulated and two down-regulated DEGs encoding for CaM-like (CML) proteins (Additional file 3: Table S2). In addition, there were two up-regulated and two down-regulated DEGs for calcium-transporting ATPase proteins, two up-regulated and one down-regulated DEGs for calcium-dependent protein kinases (CDPKs), and one down-regulated DEG for calcineurin B-like-interacting protein kinase (CIPK).

For phytohormones associated with defense signaling, there were four up-regulated and three down-regulated DEGs related to JA, four up-regulated and eight down-regulated DEGs related to lipoxygenase (LOX), four up-regulated and four down-regulated DEGs related to ethylene (ET), and three up-regulated and two down-regulated DEGs related to salicylic acid (SA) synthesis and degradation (Additional file 3: Table S2). The results showed that JA, LOX, ET and SA might be involved, but with more genes associated with LOX rather than JA, ET or SA. Furthermore, there were two down-regulated DEGs related to allene oxide synthase (AOS) and one down-regulated DEG related to acetyl-CoA carboxylase (ACC) synthesis.

Analysis of DEGs involved in cell wall reorganization

Among the 75 cell-wall-related DEGs (Additional file 4: Table S3), there were more down-regulated than up-regulated DEGs for xyloglucan xyloglucosyltransferase (8 down vs 1 up), alpha-glucosidases (19 down vs 5 up), beta-glucosidases (13 down vs 2 up) and endo-13-beta-glucosidase (15 down vs 7 up). There were two down-regulated xyloglucan endotransglycosylase and one down-regulated callose synthase 3. Only invertase/pectin methylesterase inhibitor had a similar number of up- and down-regulated DEGs (1 down vs 1 up), and there were no cell-wall-related DEGs with more up-regulated than down-regulated DEGs. These results indicate the degree to which cell wall enzyme activity was down-regulated during *Ggt* infection.

Analysis of DEGs for pathogenesis-related (PR) proteins

Among the 23 DEGs assigned as PR proteins, 15 were up-regulated and 8 were down-regulated in response to *Ggt* infection (Table 2). Although more PR protein-coding genes were up-regulated than those down-regulated by *Ggt* infection, this varied considerably between PR families. The two PR1 family members were down-regulated. Among the three PR2 members, two were up-regulated but one was down-regulated. For the eight PR3 DEGs, six were up-regulated while two were down-regulated. One belonged to the PR4 family and

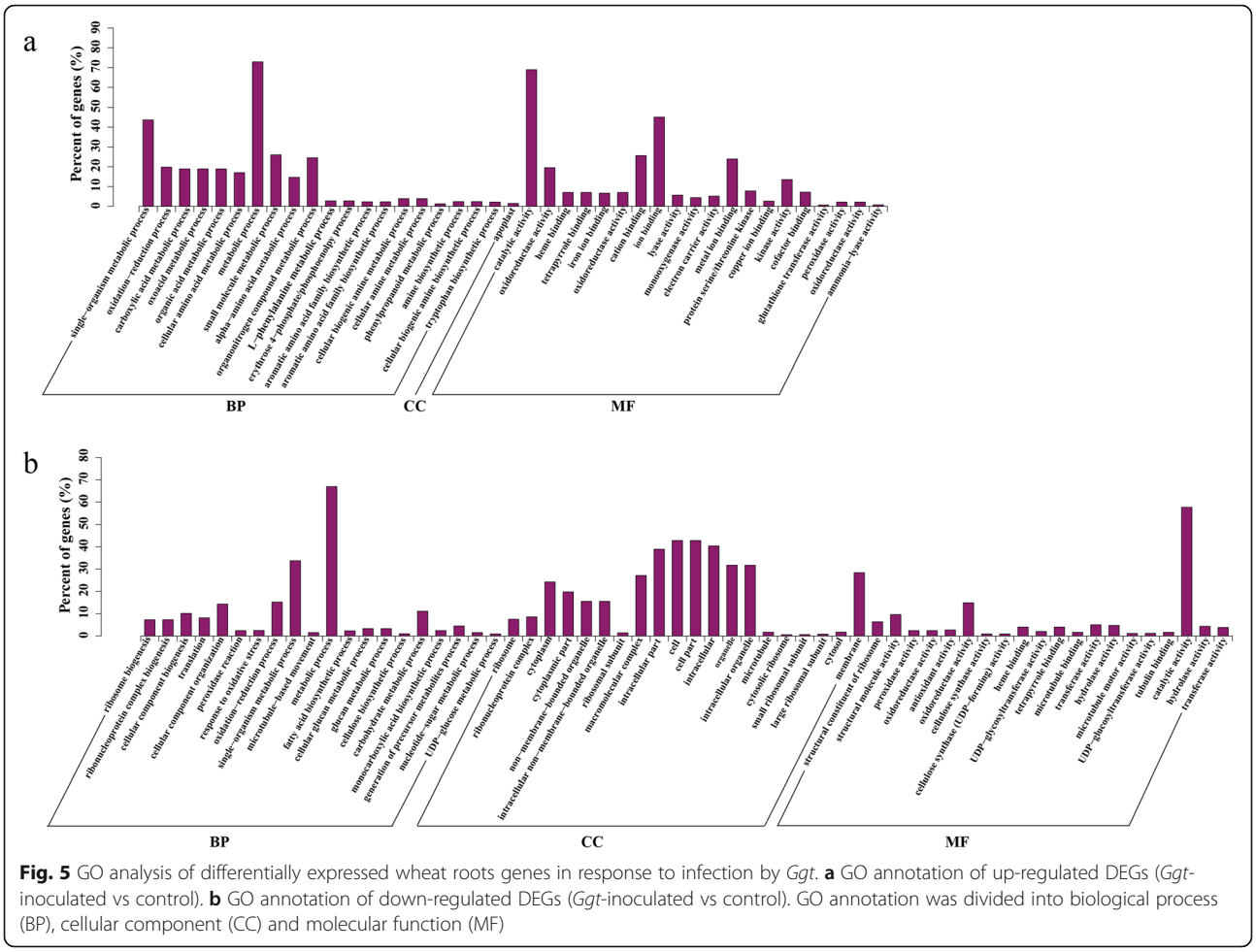

Fig. 5 GO analysis of differentially expressed wheat roots genes in response to infection by *Ggt*. **a** GO annotation of up-regulated DEGs (*Ggt*-inoculated vs control). **b** GO annotation of down-regulated DEGs (*Ggt*-inoculated vs control). GO annotation was divided into biological process (BP), cellular component (CC) and molecular function (MF)

was up-regulated; four belonged to the thaumatin/osmotin PR5 family of which three were up-regulated and one was down-regulated; one belonged to PR6 family and was down-regulated; three belonged to the PR10 family of which two were up-regulated and one was down-regulated; and one belonged to the PR1–17 family and was up-regulated. This indicates that comparatively few *PR1*, *PR4*, *PR6* and *PR1–17* genes play roles in the host response compared to the *PR2*, *PR3*, *PR5* and *PR10* genes.

Validation of transcriptomics data by RT-qPCR

In order to confirm the accuracy and reproducibility of the transcriptome analysis results, 11 randomly selected up-regulated DEGs and 2 randomly selected down-regulated DEGs (*LOX2* and *GLU*) in response to *Ggt* infection were tested by RT-qPCR using independently collected samples, which were at the same developmental stage as those used for RNA-seq (Fig. 6). A comparison of the FPKM values of all the DEGs in the RNA-seq data showed similar expression patterns between the *Ggt*-inoculated and control plants in the RT-qPCR assays.

A time-course analysis of gene expression was performed (Additional file 5: Figure S2). Most of these genes showed relatively low expression in control roots relative to that observed in *Ggt*-inoculated roots with little to no major changes over time, except for *MAPK* and *GLU*. *MAPK* had a relatively stable and high expression in control roots with a slight decline at 6–8 dpi, while *GLU* had a fluctuating expression over time with a peak at 4 dpi.

In *Ggt*-inoculated roots, all these genes showed changes in expression profile after pathogen inoculation (Fig. S2). *LOX*2 had a unique expression pattern in that it progressively declined after inoculation. The expression of one group of genes (*LOX7, MAPK, POD3–1* and SA synthesis-related genes) reached a peak at 3–4 dpi, which was prior to the appearance of root symptom. Among those, *MAPK* was unique in that its expression from 6 to 8 dpi was down-regulated compared to the control. The expression of another group of genes (*TaKSL2, WRKY4, WRKY10* and *PR4*) showed a peak at 5–6 dpi, which was around the time point of lesion appearance. The two PR protein-encoding genes (*PR1–17*

Table 1 DEGs involved in defense regulation

Category	Annotation	DEG number	Gene ID in Nr database	Gene ID in ***Triticum aestivum***	Log_2 FC
WRKY transcription factors	WRKY 2 protein	comp86043_c0	CAH68818.1	TraesCS7B02G419400.1	5.0487
	WRKY 72 transcription factor	comp86066_c0	BAJ99245.1	TraesCS3D02G113300.1	3.7098
	WRKY 27 transcription factor	comp86495_c1	ACD80363.1	TraesCS3A02G347500.1	2.7197
	WRKY 4 transcription factor	comp86671_c0	ACD80365.1	TraesCS6D02G136200.1	2.684
	WRKY 6 transcription factor	comp88617_c1	BAJ96003.1	TraesCS3A02G167200.1	2.6163
	WRKY 35 transcription factor	comp89402_c2	CAE03935.3	TraesCS2D02G443000.1	−2.5933
	WRKY 61 transcription factor	comp90037_c0	BAD68776.1	TraesCS7A02G096500.1	3.3448
	WRKY10 transcription factor	comp79173_c0	ABN43182.1	TraesCS3A02G111200.1	4.1723
MAPK pathway	MAPK related serine/threonine protein kinase	comp81413_c0	ABW84007.1	TraesCS6D02G245500.1	−1.0151
	Activation of MAPK kinase activity	comp89654_c0	BAJ85327.1	TraesCS5D02G186200.1	−2.1172
	MAPK 9	comp85414_c0	BAJ92365.1	TraesCS1B02G452200.1	−1.5826
	MAPK	comp81964_c0	ABS11090.1	TraesCS4D02G198600.1	1.6246
	MAPK kinase 1	comp74716_c0	CAA66278.1	TraesCSU02G146600.1	8.7973
	MAPK kinase kinase A	comp79865_c0	BAJ97064.1	TraesCS3A02G255700.1	6.9422
	MAPK 17	comp87212_c0	XP_003565869.1	TraesCS1A02G415300.1	−1.7576

Table 2 DEGs for pathogenesis-related proteins

Category	Annotation	DEG number	Gene ID in Nr database	Gene ID in ***Triticum aestivum***	log_2 FC
PR1	Pathogenesis-related protein PR-1	comp76291_c0	BAK01216.1	TraesCS6D02G329200.1	−3.2685
	Pathogenesis-related protein PR-1-like	comp76456_c0	XP_003572884.1	TraesCS6B02G377700.1	−4.8717
PR2	β-1,3-glucanase	comp86614_c0	AAY96422.1	TraesCS3A02G486000.1	2.0349
	β-1,3-glucanase precursor	comp71573_c0	AAD28734.1	TraesCS3D02G475200.1	5.8156
	β-1,3-glucanase	comp87816_c0	ACF33176.1	TraesCS7A02G378100.1	−1.8606
PR3	Endochitinase Class III	comp64051_c0	AET86622.2	TraesCS1B02G368300.1	12.416
	Chitinase IV precursor	comp73940_c1	AAD28733.1	TraesCS2B02G369100.1	3.2264
	Chitinase class I	comp74327_c0	BAB82472.1	TraesCS2D02G033100.1	1.5759
	Chitinase class I	comp74500_c1	XP_003566595.1	TraesCS1A02G082400.1	−2.5676
	Chitinase class I	comp78928_c0	XP_003578351.1	TraesCS5A02G272400.1	−2.9105
	Chitinase class I	comp79821_c0	ACJ68105.1	TraesCS1D02G207100.1	1.7993
	Chitinase class I	comp83093_c1	BAK08163.1	TraesCS2A02G350700.1	1.4699
	Chitinase class I	comp85318_c0	CAA53626.1	TraesCS3D02G260300.1	4.4422
PR4	Pathogenesis-related protein 4a	comp75310_c0	O64392.1	TraesCS3D02G524700.1	4.1812
PR5	Thaumatin-like protein	comp68179_c0	XP_003571622.1	TraesCS5A02G018300.1	3.6306
	Thaumatin-like protein	comp74716_c0	CAA66278.1	TraesCSU02G146600.1	8.7973
	Thaumatin-like protein	comp75220_c0	P32937.1	TraesCS7D02G551400.1	4.5162
	Thaumatin-like protein TLP7	comp85387_c0	BAJ93470.1	TraesCS3B02G332200.1	−1.9375
PR6	Proteinase inhibitor	comp71270_c0	CAB71340.2	TraesCS1B02G035100.1	−1.8608
PR10	Pathogenesis-related protein 10	comp72609_c0	AAP04429.1	TraesCS5A02G090600.1	10.234
	Pathogenesis related protein 10	comp83864_c2	ACG68733.1	TraesCS2D02G317800.1	1.4221
	Pathogenesis-related protein 10	comp78426_c0	BAJ94442.1	TraesCS1A02G191700.1	−2.7291
PR1–17	Pathogenesis-related protein 1–17	comp80664_c0	AEH25632.1	TraesCS7D02G201400.1	5.5433

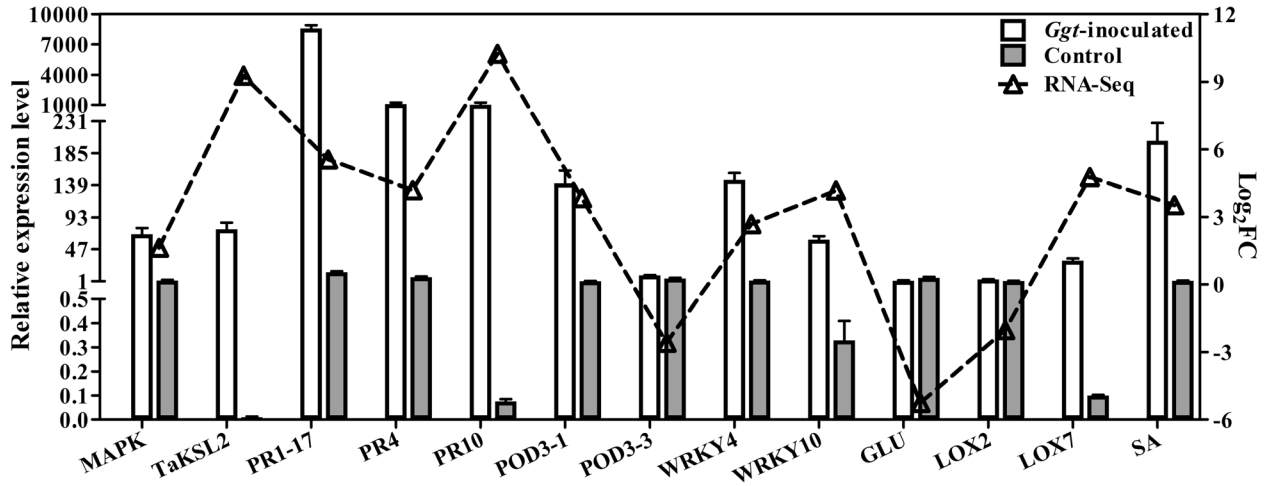

Fig. 6 Comparison of measurements of gene expression of selected DEGs by RT-qPCR and RNA-seq. Bars with standard errors represent the relative expression level of DEGs determined by RT-qPCR using the $2^{-\Delta\Delta CT}$ method from three biological replicates in three independent experiments (left Y-axis). Columns in white represent *Ggt*-inoculated samples, and columns in gray represent control samples. Broken lines indicate transcript abundance changes (log_2 fold change) based on FPKM values from RNA-Seq analysis (right Y-axis)

and *PR10*) showed a progressive increase in expression over time with a peak after the appearance of symptoms. Finally, two DEGs (*POD3–3* and *GLU*) showed a bimodal expression pattern with one peak after inoculation and the other peak at the time of lesion appearance.

Discussion

Take-all caused by *Ggt* is a destructive root disease of wheat leading to yield losses of up to 40–60% (Gutteridge et al. 2003). It is important to understand the infection process of *Ggt* in wheat roots by examining the cellular and transcriptional responses of wheat roots to *Ggt* infection. In this study, we found that the initial observable effect of *Ggt* infection on roots was reduced root growth, which occurred 2 days prior to the appearance of necrosis and rust discoloration. The timing and appearance of symptoms reported here was similar to that of previous studies using the same partially resistant wheat variety (Yang et al. 2015b). A consequence of root damage by *Ggt* is reduced leaf length and leaf chlorosis (Freeman and Ward 2004; Okagaki et al. 2016), which was observed in this study as well. Following reduced root growth, characteristic black to chocolate brown lesions appeared at 5 dpi that enlarged over time, and rust symptoms appeared at 6 dpi. Microscopical examinations showed that lesions appeared when the fungus could be detected in the endodermis, pericycle and phloem at 5 dpi, and rust symptoms corresponded to extensive colonization of the cortex region by 6 dpi. Thus, the pathogen is likely to affect gene expression in the root before necrosis is visible, and samples collected at 5 dpi were selected for RNA sequencing. At this time point, the impact of *Ggt* infection on root cells must have occurred but is not enough to cause necrosis.

GO and KEGG pathway enrichment analysis revealed significant differences between the possible functions of the up-regulated and down-regulated DEGs at 5 dpi. Some functions of the up-regulated DEGs could be connected to defense and stress responses. For example, the up-regulated DEGs related to phenylpropanoids include the cell wall defense compound lignin that has been linked to stem rust resistance in wheat (Moerschbacher et al. 1988). A take-all resistant wheat genotype was more efficient in converting phenolics to lignin, which was related to a higher resistance to take-all (Rengel et al. 1994). Other up-regulated functions were related to stilbenoids that were shown to be the major anitmicrobial phytoalexins in grapes (Malacarne et al. 2011), diterpenoids that were found to be important anitmicrobial phytoalexins in rice (Peters 2006), isoquinoline alkaloids that were demonstrated to have antifungal activity in *Fumaria* and *Corydalis* species (Orhana et al. 2007) and diarylheptanoids that were reported to possess antioxidant and cytoprotective (i.e., protection against lipid peroxidation) activities (Tao et al. 2008). In contrast, some DEGs were down-regulated during *Ggt* infection, such as cell wall reorganization-related genes, which may contribute to the reduced growth of the roots. For instance, some down-regulated DEGs encode xyloglucan endotransglycosylases, which are responsible for hydrolyzing and rejoining intermicrofibrillar xyloglucan chains and related to cell wall loosening required for plant cell expansion (Fry et al. 1992).

WRKY transcription factors are well known to play important roles in the regulation of transcriptional reprogramming associated with a variety of plant processes

but most notably with defense responses to pathogens. For example, in *Arabidopsis*, WRKY4 plays a positive role in resistance to necrotrophic pathogens but a negative role in resistance to biotrophic pathogens (Lai et al. 2008). In rice, the expression of rice *WRKY4* gene was rapidly up-regulated upon infection of the nectrotrophic fungal pathogen *Rhizoctonia solani* via the JA/ET-dependent signal pathway (Wang et al. 2015). In wheat, we found that the expression of a *WRKY4* gene was up-regulated during *Ggt* infection, which is consistent with *Ggt* being a necrotrophic pathogen. We also found that *WRKY10* expression was significantly induced by *Ggt*, which is similar to its upregulated expression in wheat crowns infected with *Fusarium pseudograminearum* (Desmond et al. 2008). Among 8 DEGs annotated as members of the *WRKY* gene family, the expression of *WRKY35* was the only one that was down-regulated. It will be important to determine whether WRKY35 is a negative regulator in wheat-*Ggt* interaction in future studies. MAPK cascades also have an important role in plant stress responses and development, and can positively regulate a wide array of defense-related responses, as demonstrated in *Arabidopsis* defense against bacteria (Anderson et al. 2011). For example, the MAPK kinase 2 mediated both the abiotic stress tolerance to cold and salt stress and biotic stress resistance to *P. syringae* pv. *tomato* (Brader et al. 2007). In wheat, we found that a MAPK kinase 1-encoding gene was strongly up-regulated in response to *Ggt* infection, and it may pay a role in regulating defense response to *Ggt* infection.

Many DEGs identified in this study are involved in SA, JA and ET signaling pathways that are known to be associated with root rot resistance (De Coninck et al. 2015). JA- and ET-mediated signaling pathways are mainly linked to plant responses to necrotrophic pathogens and herbivores, while the SA-dependent pathway is mainly involved in responses to biotrophic pathogens, and these pathways can act antagonistically (De Coninck et al. 2015; Jiang et al. 2016). Consistent with their roles in *Arabidopsis*, wheat DEGs identified in this study in response to *Ggt* include 8 up-regulated and 13 down-regulated DEGs related to JA (JA, JAZ, LOX and AOS functions), 4 up-regulated and 4 down-regulated DEGs related to ET, but only 3 up-regulated and 3 down-regulated DEGs related to SA. Additional support for a link between JA/ET signaling and *Ggt* infection was the up-regulation of a *WRKY27* gene in response to *Ggt*. In *Arabidopsis*, WRKY27 regulates the expression of genes related to ET/JA signaling in plants infected by *Ralstonia solanacearum* (Mukhtar et al. 2008). However, the importance of WRKY27 in JA/ET-mediated signaling in response to pathogen attaches remain to be characterized.

The expression of PR proteins is often used to monitor the response of plants to pathogen infection. Among DEGs encoding PR proteins identified in this study, the most significantly up-regulated one was a PR3 gene that had a 12.416-fold increase in transcript abundance, followed by a PR10 (10.234-fold), a PR5 (8.7973-fold), and a PR2 (5.8156-fold) genes. The PR3 family proteins are chitinases that act to degrade the cell wall of fungi and inhibit spore germination. The PR10 family proteins are ribonucleases conferring resistance against various stresses caused by fungi (Lee et al. 2012). The PR5 family proteins are thaumatin-like proteins acting against fungal cell membranes (Krishnaveni et al. 1999). The PR2 family proteins are β-1,3-glucanases that can hydrolyze β-1,3- glucan, a fungal cell wall component. In a microarray study of the response of wheat crowns to *F. pseudograminearum* infection, the largest class of induced genes was PR protein-encoding genes, including those for chitinase, glucanase, PR1, ribonuclease and thaumatin-like proteins (Desmond et al. 2008), demonstrating that there are similarities between wheat response to *F. pseudograminearum* and to *Ggt*, both of which are necrotrophic fungi.

Although the DEGs identified in this study were for wheat roots infected by *Ggt* at 5 dpi when root symptoms initially appeared, RT-qPCR analysis with selected DEGs showed that some of them had peaked expression at different time points corresponding to before, during, or after the appearance of lesions in roots. Thus, it will be important to identify DEGs in wheat roots at multiple time points during *Ggt* infection as well as compare differences among wheat cultivars differed in resistance against *Ggt* in future studies. Nevertheless, to our knowledge, this is the first large scale analysis of wheat root transcriptional responses against *Ggt* infection. Results from this study provides an initial view of the changes of wheat gene expression in response to *Ggt* infection, which is beneficial to improve our understanding of resistance mechanisms against take-all at the transcriptome level in wheat and possibly other cereal crops.

Conclusions

Based on the results of this study, one can hypothesize that the following series of events occurs following invasion of wheat roots by *Ggt*. First, host pattern recognition receptors were initiated to recognize MAMPs from *Ggt* hyphae as well as root DAMPs due to cell wall degrading enzymes, proteases and other secreted molecules of the fungus. This would then activate MAMP-triggered immunity. The major signaling molecules are JA and ET, but SA also appears to be involved. Eventually, gene expression would be affected by transcription factors, such as WRKY10. Major defense response corresponding to this process mainly includes lignification and production of antimicrobial proteins, such as a range of different PR proteins, and antimicrobial

compounds, like diterpenoids. These would limit the invasion by *Ggt*. At the same time, some down-regulated genes were also identified, such as xyloglucan xylosyltransferase and beta-glucosidase-encoding genes, which could be related to reduced root growth as host metabolism is shifted towards defense and biotic stress responses as well as damage repairing caused by the activities of the pathogen.

Methods

Pathogen inoculation and observation

Winter wheat 'Zhengmai 366', partially susceptible to take-all pathogen, *Ggt*, was provided by the Wheat Research Institute (Henan Academy of Agricultural Sciences, Zhengzhou, China). *Ggt* was isolated from symptomatic wheat roots (Quan et al. 2014). For the preparation of *Ggt* inoculum, 100 μL *Ggt* conidial suspension (10^8 conidia/mL) was transferred to a 150 mL flask containing 50 mL PD broth and cultured at 25 °C with shaking at 150 rpm for 7 days. Hyphae were harvested by centrifugation at 12,000 rpm for 10 min, washed with three times, and resuspended in sterile distilled water to 1 mg per mL. For inoculation, wheat seeds were germinated in Petri dishes with sterile filter paper moistened with 5 mL of sterile water. Seedlings were transferred to another sterile Petri dish with filter paper and 10 mL of sterile water (50 seedlings per dish). When the root lengths were 2–3 cm, the seedlings were transferred to tissue culture vessels and inoculated with 5 mL of *Ggt* inoculum. The wheat seedlings inoculated with an equivalent amount of sterile distilled water were set as the control. All plants were grown under a photoperiod of 16 h light/8 h dark at 22 °C (Yang et al. 2015b). After pathogen inoculation, leaf and root length of wheat seedlings were respectively measured at 1–8 dpi, and meanwhile the disease symptoms in the wheat plants were observed. In addition, segments of root elongation zone in *Ggt*-infected and control wheat plants were sampled at 1–8 dpi. The samples were then co-stained with wheat-germ agglutinin-Alexa Fluor 488 conjugate (WGA-AF488) and propidium iodide (PI) (Redkar et al. 2018). WGA-AF88 stains fungal hyphae green, and the propidium iodide stains plant cell walls red. After staining, the slides were scanned and digitalized by using a Pannoramic MIDI (3DHISTECH, Budapest, Hungary) with differential epifluorescence (GFP filter set for WGA-AF488: 450–490 nm excitation, 500-550 nm emission; TX2 filter set for PI: excitation 540–580 nm, emission 608–683 nm). The image was analyzed using the program, Pannoramic Viewer (3DHISTECH).

Extraction and quality analysis of total RNA

Total RNA was extracted from root samples of *Ggt*-infected wheat and control wheat plants at 5 dpi using RNAiso Plus kit (TaKaRa, Otsu, JP). The RNA purity was evaluated with a NanoPhotometer® spectrophotometer (Implen, Westlake Village, CA, USA), and the integrity of the RNA samples was assessed using the RNA Nano 6000 Assay Kit of the Bioanalyzer 2100 system (Agilent Technologies, Wilmington, DE, USA). The RNA was finally dissolved in RNase-free water and stored at -80 °C until use.

cDNA preparation and Illumina sequencing

Total RNA was treated with DNase I to remove DNA, and magnetic beads with oligo (dT) were used to isolate mRNA. The mRNA was mixed with divalent cations in NEB Next First Strand Synthesis Reaction Buffer (5×) under elevated temperature (Yang et al. 2015b). Then cDNA was synthesized using the fragmented mRNA as template. The cDNA was purified with AMPure XP system (Beckman, Brea, CA, USA) and then dissolved in elution buffer from the manufacturer. The purified cDNA was used for end repair and single nucleotide adenine addition by exonuclease/polymerase, (NEB, Ipswich, MA, USA). Short fragments were connected with adapters by hairpin loop structure, and fragments of 150 bp to 200 bp in length were selected preferentially for PCR amplification as templates. During the quality control steps, an Agilent 2100 Bioanalyzer (Agilent Technologies, Santa Clara, CA, USA) was used to assess the quantify of sample library. Finally, the library was sequenced using the Illumina HiSeq 2000 (Novogene, Beijing, CN). After sequencing, raw reads containing sequencing adapters and low-quality reads were removed (Zhao et al. 2013). Transcriptome assembly was accomplished using Trinity (Grabherr et al. 2011) with theminimum_kmer_coverage set to 2 and all other parameters set to their default values. The RNA from *Ggt*-infected roots contained both wheat and *Ggt* sequences. To remove *Ggt* sequences, the reads matched *Ggt* genome (ftp://ftp.ensemblgenomes.org/pub/release-20/fungi/fasta/gaeumannomyces_graminis/dna/) were filtered. The unigenes of wheat were thus obtained and used for the following analysis.

Transcriptome annotation and analysis

To annotate the wheat unigenes, the sequences were compared to those of the NCBI non-redundant protein database (Nr) by using the BLASTx algorithm with an *e*-value threshold of 10^{-5}. Selected unigenes were then mapped to the wheat genome (ftp://ftp.ensemblgenomes.org/pub/plants/release-47/fasta/triticum_aestivum/cdna/). The results of gene annotation were shown in Additional file 6: Table S4. Prior to differential gene expression analysis for each sequenced library, the read counts were adjusted using the Edge R program package (Novogene, Beijing, CN) through one scaling normalized

factor. Sequence splicing and redundancy was determined by RSEM software (Li and Dewey 2011). Unigenes with < 20 total reads were not included in the analysis. Then the DEGs were identified from the FPKM (expected number of fragments per kilobase of transcript sequence per milions base pairs sequenced) values (Trapnell et al. 2010) using the DEGseq R package (Wang et al. 2010). *P* value was adjusted using the q value, and the q value < 0.005 and $|\log_2(\text{fold change})| > 1$ was set as the threshold for significantly differential expression (Wang et al. 2010). The FPKM values in *Ggt*-inoculated and control roots were shown in Additional file 7: Table S5, and the $\log_2$ fold change values from read counts in *Ggt*-inoculated and control roots were shown in Additional file 8: Table S6.

The up-regulated and down-regulated DEGs were separated based on hierarchical clustering using the $\log_{10}$ (FPKM+ 1) values by the pheatmap package (http://www.plob.org/), Gene Ontology (GO) and Kyoto Encyclopedia of Gene and Genomes (KEGG) pathways. In the hierarchical clustering analysis, a DEG was considered to be highly expressed if the normalized data > 0. Conversely, a DEG was considered to be lowly expressed if the normalized data < 0. The level of gene expression was visualized by using a color gradient from dark blue (low expression) to dark red (high expression) (van Aerle et al. 2013). GO enrichment analysis (http://www.geneontology.org) of the DEGs was implemented by the GOseq R packages (Young et al. 2010), and the corrected *P*-value < 0.05 was set as the threshold for GO analysis. KEGG is a database resource for understanding high-level functions and utilities of the biological system, such as the cell, the organism and the ecosystem, from molecular-level information, especially large-scale molecular datasets generated by genome sequencing and other high-throughput experimental technologies (Kanehisa et al. 2008) (http://www.genome.jp/kegg/). We used KOBAS software (Mao et al. 2005) to test the statistical enrichment of DEGs in KEGG pathways. For results of KEGG pathways, see Additional file 9: Table S7.

RT-qPCR assay

RT-qPCR assays were performed to validate RNA-seq results with independent samples of *Ggt*-inoculated and control wheat roots under the same conditions as those used for RNA-Seq analysis. cDNAs were reversely transcribed using Prime Script RT reagent Kit with gDNA Eraser (Takara, Otsu, JP), and RT-qPCR analyses were performed on an Step One Plus Real-Time PCR System (Applied Biosystems, Foster City, CA, USA) using SYBR Premix Ex *Taq* (Tli RNaseH Plus) (Takara, Otsu, JP). The wheat gene, *RLI* (RNase L inhibitor-like protein) (Giménez et al. 2011), was used as an internal control to normalize the expression data. Gene expression was evaluated by the $2^{-\Delta\Delta Ct}$ method (Livak and Schmittgen 2001). The gene-specific primers are listed in Additional file 10: Table S8.

Accession numbers

All RNA-seq data have been submitted to the NCBI Sequence Read Archive (SRA) (http://www.ncbi.nlm.nih.gov/sra/) under the accession number SRR5165156.

Supplementary information

Supplementary information accompanies this paper at https://doi.org/10.1186/s42483-020-00066-7.

Additional file 1: Table S1. Summary of RNA-Seq data sets.

Additional file 2: Figure S1. a KEGG annotation of up-regulated DEGs. **b** KEGG annotation of down-regulated DEGs. The y-axis corresponds to KEGG pathway, and the x-axis shows the enrichment factor. The q value indicates adjusted *p* value, and the closer to zero the q value, the more significant the enrichment. The color of the dot represents the q value, and the size of the dot represents the number of DEGs mapped to the reference pathways.

Additional file 3: Table S2. DEGs involved in signal transduction pathways.

Additional file 4: Table S3. DEGs involved in cell wall reorganization.

Additional file 5: Figure S2. Time course of expression of selected DEGs in *Ggt*-inoculated (black bar) and control (gray bar) wheat roots at 1, 2, 3, 4, 5, 6, 7 and 8 dpi. Gene expression was measured by RT-qPCR with the wheat *RLI* gene as an internal control to normalize the expression data. The bars represent the standard deviation from three independent experiments with three replicates each.

Additional file 6: Table S4. The results of gene annotation. (XLS 36519 kb)

Additional file 7: Table S5. The FPKM values in *Ggt*-inoculated and healthy control wheat roots. (XLS 9033 kb)

Additional file 8: Table S6. The $\log_2$ fold change values from readcounts in *Ggt*-inoculated and healthy control wheat roots. (XLS 568 kb)

Additional file 9: Table S7. The KEGG pathways in *Ggt*-inoculated and healthy control wheat roots. (XLS 91 kb)

Additional file 10: Table S8. The gene-specific primers used for RT-qRCR.

Abbreviations

ACC: Acetyl-CoA carboxylase; AOS: Allene oxide synthase; BP: Biological process; CaM: Calmodulin; CC: Cellular component; CDPKs: Calcium-dependent protein kinases; CML: CaM-like; CIPK: Calcineurin B-like-interacting protein kinase; DAMPs: Damage associated molecular patterns; DEGs: Differentially expressed genes; ET: Ethylene; FPKM: Expected number of fragments per kilobase of transcript sequence per milions base pairs sequenced; *Ggt*: *Gaeumannomyces graminis* var. *tritici*; GO: Gene Ontology; JA: Jasmonic acid; KEGG: Kyoto Encyclopedia of Gene and Genomes; LOX: Lipoxygenase; MAMPs: Microbe-associated molecular patterns; MAPK: Mitogen-activated protein kinase; MF: Molecular function; Nr: Non-redundant protein database; PI: Propidium iodide; PR: Pathogenesis-related; RT-qPCR: Reverse transcription quantitative PCR; RLI: RNase L inhibitor-like protein; RNA-Seq: RNA sequencing; SA: Salicylic acid; WGA-AF488: Wheat germ agglutinin-Alexa Fluor 488 conjugate

Acknowledgements

The authors would like to thank Prof. Jinrong Xu and Prof. Cong Jiang (Northwest A&F University) for critical reading of the manuscript. We also thank Dr. Wen Xu (Henan Academy of Agricultural Sciences) for his help with data analysis.

Authors' contributions
LY and JZ conceived and designed the experiments. JZ, HY, MX, XH and LX carried out the experiments. All authors analyzed the data. JZ, HY and XH drafted the manuscript. LY, XQ, RS and PG revised the manuscript. All authors read and approved the final manuscript.

Funding
This work was supported by grants from the National Key Research and Development Program of China (2017YFD0200901), National Natural Science Foundation of China (31401815), Major Achievement Cultivation Program of Henan Academy of Agricultural Sciences (20191101004), the Central Government Guide Local Projects (2020[44]).

Availability of data and materials
Not applicable.

Ethics approval and consent to participate
Not applicable.

Consent for publication
Not applicable.

Competing interests
The authors declare that they have no competing interests.

Author details
[1]Institute of Plant Protection Research, Henan Academy of Agricultural Sciences, Henan Biopesticide Engineering Research Center, Henan International Joint Laboratory of Crop Protection, Zhengzhou 450002, P. R. China. [2]Hohhot Environmental Monitoring Center, Hohhot 010030, P. R. China. [3]School of Chemical and Environmental Engineering, Pingdingshan University, Pingdingshan 467000, P. R. China. [4]School of Environmental Sciences, University of Guelph, Guelph, Canada.

Received: 16 March 2020 Accepted: 5 August 2020
Published online: 14 August 2020

References

Anderson JC, Bartels S, González BMA, Shahollari B, Ulm R, Peck SC. *Arabidopsis* MAP kinase phosphatase 1 (AtMKP1) negatively regulates MPK6-mediated PAMP responses and resistance against bacteria. Plant J. 2011;67:258–68.
Bertini L, Caporale C, Testa M, Proietti S, Caruso C. Structural basis of the antifungal activity of wheat PR4 proteins. FEBS Lett. 2009;583:2865–71.
Brader G, Djamei A, Teige M, Palva ET, Hirt H. The MAP kinase kinase MKK2 affects disease resistance in *Arabidopsis*. Mol Plant-Microbe Interact. 2007;20:589–96.
Browse J. The power of mutants for investigating jasmonate biosynthesis and signaling. Phytochemistry. 2009;70:1539–46.
Chand SK, Nanda S, Rout E, Mohanty JN, Mishra R, Joshi RK. De novo sequencing and characterization of defense transcriptome responsive to *Pythium aphanidermatum* infection in *Curcuma longa* L. Physiol Mol Plant Pathol. 2016;94:27–37.
Cook RJ. Take-all of wheat. Physiol Mol Plant Pathol. 2003;62:73–86.
De Coninck B, Timmermans P, Vos C, Cammue BPA, Kazan K. What lies beneath: belowground defense strategies in plants. Trends Plant Sci. 2015;20:91–101.
Desmond OJ, Manners JM, Schenk PM, Maclean DJ, Kazan K. Gene expression analysis of the wheat response to infection by *Fusarium pseudograminearum*. Physiol Mol Plant Pathol. 2008;73:40–7.
Fang WP, Zhao FA, Sun Y, Xie DY, Sun L, Xu ZZ, et al. Transcriptomic profiling reveals complex molecular regulation in cotton genic male sterile mutant Yu98-8A. PLoS One. 2015;18:e0133425.
Freeman J, Ward E. *Gaeumannomyces graminis*, the take-all fungus and its relatives. Mol Plant Pathol. 2004;5:235–52.
Fry SC, Smith RC, Renwick KF, Martin DJ, Hodge SK, Matthews KJ. *Xyloglucan endotransglycosylase*, a new wall-loosening enzyme activity from plants. Biochem J. 1992;282:821–8.
Giménez MJ, Pistón F, Atienza SG. Identification of suitable reference genes for normalization of qPCR data in comparative transcriptomics analyses in the *Triticeae*. Planta. 2011;233:163–73.
Glazebrook J. Contrasting mechanisms of defense against biotrophic and necrotrophic pathogens. Annu Rev Phytopathol. 2005;43:205–27.
Grabherr MG, Haas BJ, Yassour M, Levin JZ, Thompson DA, Amit I, et al. Full-length transcriptome assembly from RNA-Seq data without a reference genome. Nat Biotechnol. 2011;29:644–52.
Guilleroux M, Osbourn A. Gene expression during infection of wheat roots by the 'take-all' fungus *Gaeumannomyces graminis*. Mol Plant Pathol. 2004;5:203–16.
Gutteridge RJ, Bateman GL, Todd AD. Variation in the effects of take-all disease on grain yield and quality of winter cereals in field experiments. Pest Manag Sci. 2003;59:215–24.
Jiang YZ, Guo L, Liu R, Jiao B, Zhao X, Ling ZY, et al. Overexpression of poplar *PtrWRKY89* in transgenic *Arabidopsis* leads to a reduction of disease resistance by regulating defense-related genes in salicylate- and jasmonate-dependent signaling. PLoS One. 2016;11:e0149137.
Kanehisa M, Araki M, Goto S, Hattori M, Hirakawa M, Itoh M, et al. KEGG for linking genomes to life and the environment. Nucleic Acids Res. 2008;36:D480–4.
Koornneef A, Pieterse CMJ. Cross talk in defense signaling. Plant Physiol. 2008;146:839–44.
Krishnaveni S, Muthukrishnan S, Liang GH, Wilde G, Manickam A. Induction of chitinases and β-1,3-glucanases in resistant and susceptible cultivars of sorghum in response to insect attack, fungal infection and wounding. Plant Sci. 1999;144:9–16.
Kwak YS, Bakker PAHM, Glandorf DCM, Rice JT, Paulitz TC, Weller DM. Diversity, virulence, and 2,4-diacetylphloroglucinol sensitivity of *Gaeumannomyces graminis* var. *tritici* isolates from Washington state. Phytopathology. 2009;99:472–9.
Lai ZB, Vinod KM, Zheng ZY, Fan BF, Chen ZX. Roles of *Arabidopsis* WRKY3 and WRKY4 transcription factors in plant responses to pathogens. BMC Plant Biol. 2008;8:68.
Lee OR, Pulla RK, Kim YJ, Balusamy SRD, Yang DC. Expression and stress tolerance of *PR10* genes from *Panax ginseng* C. A. Meyer. Mol Biol Rep. 2012;39:2365–74.
Li B, Dewey CN. RSEM: accurate transcript quantification from RNA-Seq data with or without a reference genome. BMC Bioinf. 2011;12:323.
Li XY, Gao L, Zhang WH, Liu JK, Zhang YJ, Wang HY, et al. Characteristic expression of wheat *PR5* gene in response to infection by the leaf rust pathogen, *Puccinia triticina*. J Plant Interact. 2015;10:132–41.
Livak KJ, Schmittgen TD. Analysis of relative gene expression data using real-time quantitative PCR and the $2^{-\Delta\Delta Ct}$ method. Methods. 2001;25:402–8.
Malacarne G, Vrhovsek U, Zulini L, Cestaro A, Stefanini M, Mattivi F, et al. Resistance to *Plasmopara viticola* in a grapevine segregating population is associated with stilbenoid accumulation and with specific host transcriptional responses. BMC Plant Biol. 2011;11:114.
Mao XZ, Cai T, Olyarchuk JG, Wei LP. Automated genome annotation and pathway identification using the KEGG Orthology (KO) as a controlled vocabulary. Bioinformatics. 2005;21:3787–93.
Mattiacci L, Dicke M, Posthumus MA. β-Glucosidase: an elicitor of herbivore-induced plant odor that attracts host-searching parasitic wasps. Proc Natl Acad Sci USA. 1995;92:2036–40.
Mcmillan VE, Gutteridge RJ, Hammond-Kosack KE. Identifying variation in resistance to the take-all fungus, *Gaeumannomyces graminis*. var. *tritici*, between different ancestral and modern wheat species. BMC Plant Biol. 2014;14:212.
Moerschbacher BM, Noll UM, Flott BE, Reisener HJ. Lignin biosynthetic enzymes in stem rust infected, resistant and susceptible near-isogenic wheat lines. Physiol Mol Plant Pathol. 1988;33:33–46.
Mooney BP, Miernyk JA, Greenlief CM, Thelen JJ. Using quantitative proteomics of *Arabidopsis* root sand leaves to predict metabolic activity. Physiol Plant. 2006;128:237–50.
Mukhtar MS, Deslandes L, Auriac MC, Marco Y, Somssich IE. The Arabidopsis transcription factor WRKY27 influences wilt disease symptom development caused by *Ralstonia solanacearum*. Plant J. 2008;56:935–47.
Okagaki LH, Sailsbery JK, Eyre AW, Dean RA. Comparative genome analysis and genome evolution of members of the *Magnaporthaceae* family of fungi. BMC Genomics. 2016;17:135.
Orhana I, Özçelik B, Karaoğlu T, Sener B. Antiviral and antimicrobial profiles of selected isoquinoline alkaloids from *Fumaria* and *Corydalis* species. Z Naturforsch C J Biosci. 2007;62:19–26.
Peters RJ. Uncovering the complex metabolic network underlying diterpenoid phytoalexin biosynthesis in rice and other cereal crop plants. Phytochemistry. 2006;67:2307–17.
Quan X, Xue BG, Yang LR, Wu C. Isolation and variety identification of *Gaeumannomyces graminis* causing wheat take-all in Henan Province. Acta

Phytopathol Sin. 2014;44:139–46 (in Chinese). http://zwblxb.magtech.com.cn/CN/abstract/abstract442.shtml.
Redkar A, Jaeger E, Doehlemann G. Visualization of growth and morphology of fungal hyphae in planta using WGA-AF488 and propidium iodide co-staining. Bio-Protocol. 2018;8:1–7. https://doi.org/10.21769/BioProtoc.2942.
Rengel Z, Graham RD, Pedler JF. Time-course of biosynthesis of phenolics and lignin in roots of wheat genotypes differing in manganese efficiency and resistance to take-all fungus. Ann Bot. 1994;74:471–7.
Sang MK, Kim JG, Kim KD. Biocontrol activity and induction of systemic resistance in pepper by compost water extracts against *Phytophthora capsici*. Phytopathology. 2010;100:774–83.
Sherif S, Paliyath G, Jayasankar S. Molecular characterization of peach PR genes and their induction kinetics in response to bacterial infection and signaling molecules. Plant Cell Rep. 2012;31:697–711.
Shin SB, Lv JY, Fazio G, Mazzola M, Zhu YM. Transcriptional regulation of ethylene and jasmonate mediated defense response in apple (*Malus domestica*) root during *Pythium ultimum* infection. Hortic Res. 2014;1:14053.
Tao QF, Xu Y, Lam RYY, Schneider B, Dou H, Leung PS, et al. Diarylheptanoids and a monoterpenoid from the rhizomes of *Zingiber officinale*: antioxidant and cytoprotective properties. J Nat Prod. 2008;71:12–7.
Trapnell C, Williams BA, Pertea G, Mortazavi A, Kwan G, van Baren MJ, et al. Transcript assembly and quantification by RNA-Seq reveals unannotated transcripts and isoform switching during cell differentiation. Nat Biotechnol. 2010;28:511–5.
van Aerle R, Lange A, Moorhouse A, Paszkiewicz K, Ball K, Johnston BD, et al. Molecular mechanisms of toxicity of silver nanoparticles in zebrafish embryos. Environ Sci Technol. 2013;47:8005–14.
Wang HH, Meng J, Peng XX, Tang XK, Zhou PL, Xiang JH, et al. Rice WRKY4 acts as a transcriptional activator mediating defense responses toward *Rhizoctonia solani*, the causing agent of rice sheath blight. Plant Mol Biol. 2015;89:157–71.
Wang LK, Feng ZX, Wang X, Wang XW, Zhang XG. DEGseq: an R package for identifying differentially expressed genes from RNA-seq data. Bioinformatics. 2010;26:136–8.
Wang Z, Zhang JB, Jia CH, Liu JH, Li YQ, Yin XM, et al. De novo characterization of the banana root transcriptome and analysis of gene expression under *Fusarium oxysporum* f. sp. *cubense* tropical race 4 infection. BMC Genomics. 2012;13:650.
Weller DM. Biological control of soilborne plant pathogens in the rhizosphere with bacteria. Annu Rev Phytopathol. 1988;26:379–407.
Weller DM, Raaijmakers JM, Gardener BBM, Thomashow LS. Microbial populations responsible for specific soil suppressiveness to plant pathogens. Annu Rev Phytopathol. 2002;40:309–48.
Yang LR, Quan X, Xue BG, Goodwin PH, Lu SB, Wang JH, et al. Isolation and identification of *Bacillus subtilis* strain YB-05 and its antifungal substances showing antagonism against *Gaeumannomyces graminis* var. *tritici*. Biol Control. 2015a;85:52–8.
Yang LR, Xie LH, Xue BG, Goodwin PH, Quan X, Zheng CL, et al. Comparative transcriptome profiling of the early infection of wheat roots by *Gaeumannomyces graminis* var *tritici*. PLoS One. 2015b;10:e0120691.
Young MD, Wakefield MJ, Smyth GK, Oshlack A. Gene ontology analysis for RNA-seq: accounting for selection bias. Genome Biol. 2010;11:R14.
Zhao CZ, Waalwijk C, de Wit PJGM, Tang DZ, van der Lee T. RNA-Seq analysis reveals new gene models and alternative splicing in the fungal pathogen *Fusarium graminearum*. BMC Genomics. 2013;14:21.
Zuluaga AP, Solé M, Lu HB, Góngora-Castillo E, Vaillancourt B, Coll N, et al. Transcriptome responses to *Ralstonia solanacearum* infection in the roots of the wild potato *Solanum commersonii*. BMC Genomics. 2015;16:246.